2010 *KSME International Journal, Vol. 17 No. 12, pp. 2010~2018, 2003*

A Numerical Analysis of Molten Steel Flow Under Applied Magnetic Fields in Continuous Casting

Teuk Myo Yoon
Mechanical Engineering Department, Graduate School of Kyunghee University, Yongin 449-701, Korea
Chang Nyung Kim*
College of Mechanical & Industrial System Engineering, Kyunghee University, Yongin 449-701, Korea

Although continuous casting process has highly developed, there still remain many problems to be considered. Specifically, two vortex flows resulting from impingement against narrow walls make a flow field unstable in a mold, and it is directly related to internal and external defects of steel products. To cope with this instability, EMBR (Electromagnetic Brake Ruler) technique has been lately studied for the stability of molten steel flow, and it is revealed that molten steel flow in a mold can be controlled with applied magnetic field. However, it is still difficult to clarify flow pattern in an EMBR caster due to complex correlations among variables such as geometric factors, casting conditions, and the place and the intensity of charged magnetic field. In the present study, flow field in a mold is focused with different conditions of electromagnetic effect. To accurately analyze the case, three dimensional low Reynolds turbulent model and appropriate boundary conditions are chosen. To evaluate the electromagnetic effect in molten steel flow, dimensionless numbers are employed. The results show that the location and the intensity of the applied magnetic field significantly influence the flow pattern. Both impingement and internal flow pattern are changed remarkably with the change of the location of applied magnetic field. It turns out that an insufficient magnetic force yields adverse effect like channeling, and rather lowers the quality of steel product.

Key Words : Continuous Casting, Electromagnetic Effect, EMBR, Molten Steel Flow

Nomenclature

$\vec{B}$: Magnetic flux density
$\vec{E}$: Electric field vector
$\vec{g}$: Gravitational acceleration
$\vec{J}$: Induced current density
k : Turbulent kinetic energy
p : Pressure
$\vec{V}$: V elocity vector
y^+ : Dimensionless distance

Greek Letters

ε : Dissipation rate of turbulent kinetic energy
μ : Laminar viscosity
μ_t : Turbulent viscosity
μ_{eff} : Effective viscosity
ρ : Molten steel density
σ : Electric conductivity
φ : Electric potential

* Corresponding Author,
E-mail : cnkim@khu.ac.kr
TEL : +82-31-201-2578; **FAX** : +82-31-202-8106
College of Mechanical & Industrial System Engineering, Kyunghee University, Yongin 449-701, Korea. (Manuscript **Received** July 22, 2002; **Revised** September 30, 2003)

1. Introduction

The continuous casting process has been widely used in production of steel and nonferrous metal. And there have been intensive studies related to various parts of continuous casting processes (Li et al., 1999). Especially, molten steel flow in a

mold has been focused because flow pattern of molten steel governs the motion of inclusion particles and, mainly influences on the quality of steel. Thus, flow characteristic of molten steel in a mold is one of the most important indices for the control of slab qualities (Hwang et al., 1997; Seyedein and Hasan, 1997).

In a high speed casting, molten steel flow in a mold is featured with impingement against narrow wall and different types of two vortex flows exist caused by jet flow from a SEN(Submerged Entry Nozzle). Impingement by jet flow from the SEN yields irregular solidification on a mold wall, and entraps mold powder and steel fragments in an internal flow. After impinging against narrow wall, molten steel flow is separated into upward and downward flow (Cha and Yoon, 1999). First, upward flow hits meniscus vertically. It makes meniscus unstable and fluctuated. These instability and fluctuation cause the surface defects of steel such as oscillation marks and the entrapment of nonmetallic inclusions into the interior flow (Huang and Thomas, 1998; Cha and Yoon, 1999). Secondly, downward flow toward outlet forms large vortex flow below the SEN. The vortex flow drives deep penetration of nonmetallic inclusions into the inner part of molten flow so that internal flaws can be made in the interior of slab. Moreover, the vortex flow causes irregular flow pattern near the outlet of mold, which may allow fatal defects, like cavity and biased solidification.

In the early 1980's, to get the high quality of slabs at a high speed casting, the EMBr (Electromagnetic Braker) techniques were developed to control molten steel flow in a mold with local application of static magnetic field. However, strong channeling appeared along with narrow wall, and it lowers the quality of steel. Through many experiments and numerical analysis, EMBR (Electromagnetic Brake Ruler) and FCM (Flow Control Mold), so called the second generation EMBR technique, were successively developed in 1990's (Park et al., 1999). A number of empirical and numerical data have shown beneficial influence of EMBR technique on continuous casting processes.

In order to effectively install and run EMBR system, it is essential to understand flow pattern of molten steel in a mold with applied electromagnetic field. So far, even though many researches have been dedicated to steel flow phenomena with magnetic field, due to difficulty in the measurement of velocity field of molten steel in a mold and the management of charged electromagnetic field, detailed flow characteristics of molten steel have not been understood well (Lai et al., 1986; Zheng et al., 2001). Therefore, more extensive studies should be required to understand flow pattern of molten steel with electromagnetic effect.

In this study, two cases of molten steel flow with differently applied DC electromagnetic field in a mold have been modeled and numerically simulated in order to predict the electromagnetic effect on molten steel flow and to find the correlation between molten steel flow and the intensity and charged places of magnetic field.

2. Method of Numerical Analysis

2.1 Mathematical modeling

Two physical schematics of molten steel flow with DC magnetic field differently placed are illustrated as Fig 1. In the present study, a twin-ported submerged entry nozzle is chosen and a rectangular SEN shape is considered in the computational grid.

2.1.1 Assumptions of modeling

The following assumptions are set up for numerical analysis:

a. The molten steel is under three-dimensional turbulent flow in a steady state.
b. The molten steel flows as an incompressible Newtonian fluid.
c. Meniscus is flat and maintained at a fixed level.
d. Meniscus is covered with a nonmetallic slag layer with free surface insulated electrically.
e. As the thickness of solidifying shell is less than 10 mm when the strand leaves the mold in the steel case, solidifying shell is zero roughness.

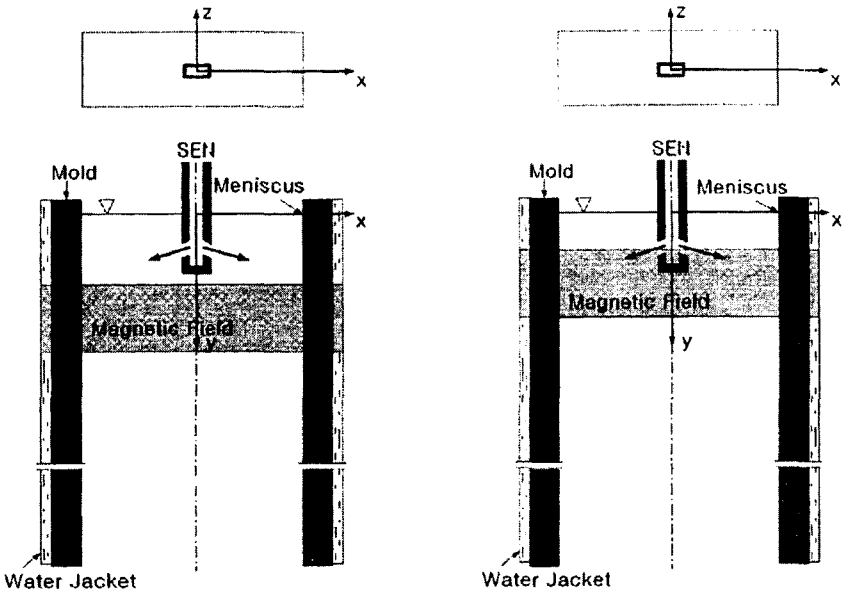

Fig. 1 The schematics of molten steel flow with differently placed magnetic field

f. Thermal properties are invariant.
g. The symmetry of molten flow is assumed so that only one quarter caster shape is considered.
h. No-slip condition is applied on the mold wall covered with mold powder.

2.1.2 Governing equations

Steady-state molten steel flow in the mold shown in Fig. 1 is governed by mass conservation, momentum conservation combined with the Lorentz force, and turbulent model equations.

Continuity equation :

$$\nabla\cdot(\rho\vec{V})=0 \tag{1}$$

Momentum equation :

$$\rho\vec{V}\cdot\nabla\vec{V}=\mu_{eff}\nabla^2\vec{V}-\nabla p+\vec{F}+\rho\vec{g} \tag{2}$$

$\vec{F}$: Lorentz force

μ_{eff} : Viscosity including laminar and turbulent viscous effect

The Lorentz force is included as a source term in the momentum equation.

$$\vec{F}=\vec{J}\times\vec{B} \tag{3}$$

where $\vec{B}$ is the intensity of an imposed magnetic field.

The current density $\vec{J}$ is given by

$$\vec{J}=\sigma(\vec{E}+\vec{V}\times\vec{B}) \text{ and } \vec{E}=-\nabla\varphi \tag{4}$$

The continuity of the induced current density is given by

$$\nabla\cdot\vec{J}=0 \tag{5}$$

hence,

$$\nabla\cdot(\sigma\nabla\varphi)=\nabla\cdot(\sigma(\vec{V}\times\vec{B})) \tag{6}$$

2.1.3 Turbulence modeling

Since the standard $k-\varepsilon$ model cannot be applied to the regions very close to the wall having low turbulent Reynolds number, low Reynolds number $k-\varepsilon$ model should be used for better prediction of flow characteristics in regions close to wall. Refined grids are required near wall, where y^+ is less than 1, to adopt low Reynolds $k-\varepsilon$ model. In this study, Chien's low Reynolds model is employed (Chien, 1982). Kinetic energy and energy dissipation equations are presented below for steady state.

$$\frac{\partial}{\partial x_j}(\rho u_j k)=\frac{\partial}{\partial x_j}\left(\left(\mu+\frac{\mu_t}{\sigma_k}\right)\frac{\partial k}{\partial x_j}\right)+\rho(P-\varepsilon-D) \quad (7)$$

$$\frac{\partial}{\partial x_j}(\rho u_j \varepsilon)=\frac{\partial}{\partial x_j}\left(\left(\mu+\frac{\mu_t}{\sigma_\varepsilon}\right)\frac{\partial \varepsilon}{\partial x_j}\right)+C_{\varepsilon 1}f_1\frac{\rho P\varepsilon}{k}-C_{\varepsilon 2}f_2\frac{\rho\varepsilon^2}{k}+E \quad (8)$$

$$\mu_t=C_\mu f_\mu\frac{\rho k^2}{\varepsilon} \quad (9)$$

$$P=\nu_t\left(\frac{\partial u_i}{\partial x_j}+\frac{\partial u_j}{\partial x_i}-\frac{2}{3}\frac{\partial u_m}{\partial x_m}\delta_{ij}\right)\frac{\partial u_i}{\partial x_j}-\frac{2}{3}k\frac{\partial u_m}{\partial x_m} \quad (10)$$

$$D=2\nu k/y^2 \quad (11)$$

$$E=-2\nu\left(\frac{\varepsilon}{y^2}\right)\exp(-0.5y^+) \quad (12)$$

$$f_\mu=1-\mathrm{ext}(-0.0115y^+) \quad (13)$$

$$f_2=1-0.22\exp\left[-\left(\frac{\mathrm{Re}_t}{6}\right)^2\right] \quad (14)$$

$$f_1=1.0$$

$$C_\mu=0.09\ ;\ C_{\varepsilon 1}=1.35\ ;\ C_{\varepsilon 2}=1.8$$

$$\sigma_k=1.0\ ;\ \sigma_\varepsilon=1.3$$

2.1.4 Boundary condition

Inlet

Considering a casting speed of 3.5 tons per minute, the inlet velocity at the SEN is given as 3.384 m/s. The kinetic energy and dissipation rate of turbulent energy at the inlet are estimated from the following semi-empirical relations (Lai et al., 1986).

$$k=0.01\times u_{inlet}{}^2 \quad (15\text{-a})$$

$$\varepsilon=0.09\times k^{1.5}/0.05/D_{nozzle} \quad (15\text{-b})$$

The gradient of electrical potential at the inlet is zero.

$$\frac{\partial\varphi}{\partial x}=0 \quad (16)$$

Free Surface

Through previous assumptions, the flat free surface is electrically insulated by nonmetallic slug layer, and the normal gradients of all variables are fixed to zero except the vertical velocities toward the free surface.

$$\frac{\partial u}{\partial y}=\frac{\partial w}{\partial y}=\frac{\partial\varphi}{\partial y}=\frac{\partial k}{\partial y}=\frac{\partial\varepsilon}{\partial y}=0,\ v=0 \quad (17)$$

Symmetry Condition

As one quarter caster shape is considered with symmetric flow of molten steel, there are two symmetry planes on x-y and y-z planes respectively.

x-y plane :

$$\frac{\partial u}{\partial z}=\frac{\partial v}{\partial z}=\frac{\partial\varphi}{\partial z}=\frac{\partial k}{\partial z}=\frac{\partial\varepsilon}{\partial z}=0,\ w=0 \quad (18)$$

y-z plane :

$$\frac{\partial v}{\partial x}=\frac{\partial w}{\partial x}=\frac{\partial\varphi}{\partial x}=\frac{\partial k}{\partial x}=\frac{\partial\varepsilon}{\partial x}=0,\ v=0 \quad (19)$$

Wall

No-slip condition and the wall insulated by mold powder are set as

x-y plane :

$$u=v=w=k=\varepsilon=0,\ \frac{\partial\varphi}{\partial z}=0 \quad (20)$$

y-z plane :

$$u=v=w=k=\varepsilon=0,\ \frac{\partial\varphi}{\partial x}=0 \quad (21)$$

Outlet

For velocities, Neumann condition is assumed. Thus, the electric potential, the turbulent energy, and the dissipation rate of turbulent energy are set to zero.

$$\frac{\partial u}{\partial y}=\frac{\partial v}{\partial y}=\frac{\partial w}{\partial y}=0,\ \varphi=k=\varepsilon=0 \quad (22)$$

2.2 Method of numerical analysis

To analyze this problem, a finite volume method is used with structured grids. The SIMPLEC algorithm is chosen to solve nonlinear equations with upwind scheme (Van doormaal and Raithby, 1984). Geometric parameters and the properties of molten steel are presented in Table 1.

Table 1 Geometrical parameters and properties of liquid steel

Parameters and Properties	Values
Mold width (m)	1.42
Mold thickness (m)	0.2383
Mold length (m)	3
Depth of the submerged entry nozzle (m)	0.12
Nozzle inside diameter (m)	0.067
Nozzle outside diameter (m)	0.0735
Nozzle cross-section area (m^2)	0.007394
Attack angle of the submerged entry nozzle	15°(downward)
Place of applied magnetic field of case 1 (m)	0.31-0.53
Place of applied magnetic field of case 2 (m)	0.16-0.44
Molten steel density (kg/m^3)	7020
Molten steel laminar viscosity ($N \cdot s/m^2$)	0.00559
Molten steel electric conductivity ($1/\Omega \cdot m$)	714000

2.3 Non-dimensional numbers

For a flow of an electrically conducting fluid where transverse magnetic effect is charged, Reynolds number and Hartmann number become important indices to estimate the interaction between viscosity and magnetic effect in the flow. Moreover, through Reynolds number and Hartmann number, Interaction parameter is gained to inform the interaction between momentum and magnetic effect.

In this study, these three non-dimensional numbers are listed below and the values of these numbers and intensity of magnetic fields are shown in Table 2.

$$\mathrm{Re}=\frac{\rho VL}{\mu} \quad : \text{Reynolds number}$$

$$\mathrm{Ha}=\sqrt{\frac{\sigma B^2 L^2}{\mu}} \quad : \text{Hartmann number}$$

$$\mathrm{I}=\frac{\sigma B^2 L}{\rho V} \quad : \text{Interaction parameter}$$

where L and V stand for mold thickness and mean downward velocity of molten steel, respectively.

Table 2 Intensities of magnetic field and non-dimensional numbers

Intensity of magnetic field & Non-dimensional number	Values			
Bz	0.1T	0.2T	0.3T	0.5T
Re	12297			
Ha	443	887	1330	2218
I	16	64	130	400

3. Results and Discussion

The molten steel flow in the mold has been numerically studied with uniformly applied magnetic field. In this study, there are two different cases with different places of the field. Each case has four different intensities of magnetic field, 0.1, 0.2, 0.3, and 0.5T. Mainly focused interests are flow fields of the following regions: around impinging point, underneath of meniscus, near the SEN, in the middle of the caster, and outlet of the mold.

Impingement against narrow wall: Near the narrow wall region, in the case 1, it is shown that the stronger magnetic field is charged, the more impinging speed is decreased, whereas, with applied magnetic field of 0. 1T, electromagnetic effect does not work sufficiently, and rather impinging speed is increased a little as shown in Fig. 2. In the case 2, the impinging speed is remarkably decreased as the intensity of magnetic field is stronger.

Underneath the free surface: In the case 1, because of the location of the applied magnetic field apart from the SEN, a part of jet flow from the SEN is reflected to the surface along with the narrow walls. The vertical velocity of molten flow steel underneath the free surface is shown in Fig. 3 and it can be reasoned that oscillation mark could be observed on the surface of slabs. In the case 2, electromagnetic effect works directly on the SEN. Compared with the case 1, impingement

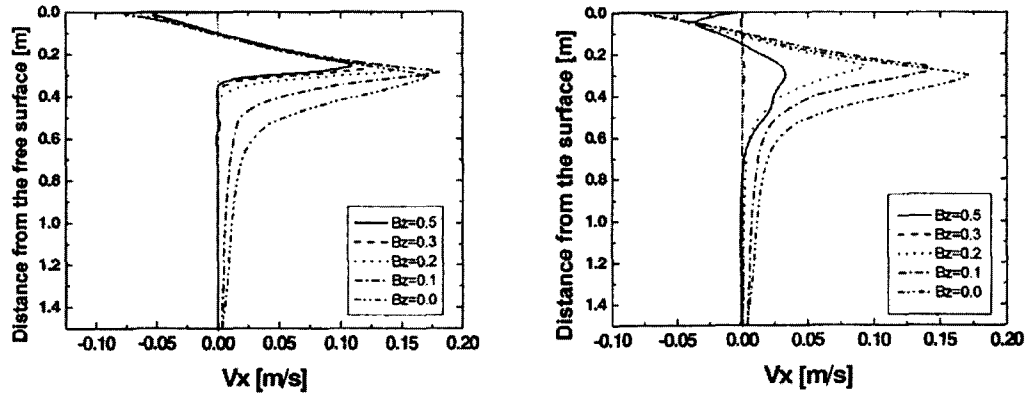

Case (1) Case (2)

Fig. 2 Velocity profiles of impinging points (x=0.69 m and z=0.0 m)

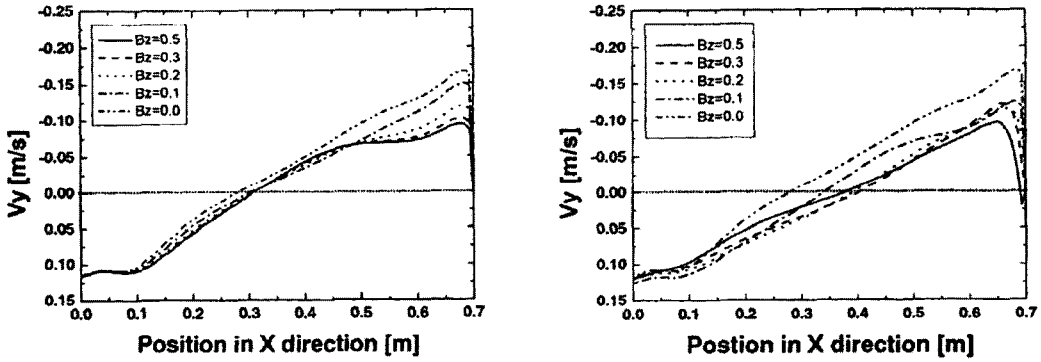

Case (1) Case (2)

Fig. 3 Velocity profiles underneath the free surface (y=0.003 m and z=0.109 m)

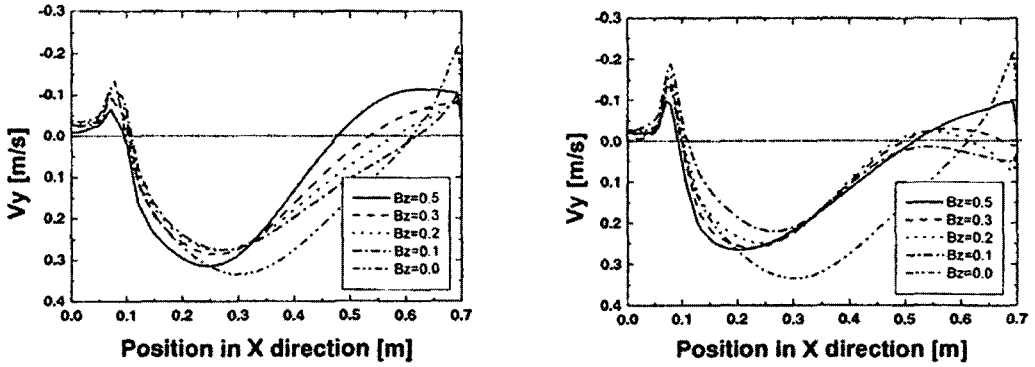

Case (1) Case (2)

Fig. 4 Velocity profiles below the SEN (y=0.275 m and z=0.0 m)

against the narrow wall becomes weak and the speed of molten steel flow toward the free surface is reduced as well. It makes possible for the free surface to be more stable.

Below the SEN : In both the cases, an eddy appears under the SEN and causes upward flow to the SEN as shown in Fig. 4. The eddy obstructs jet flow from the SEN.

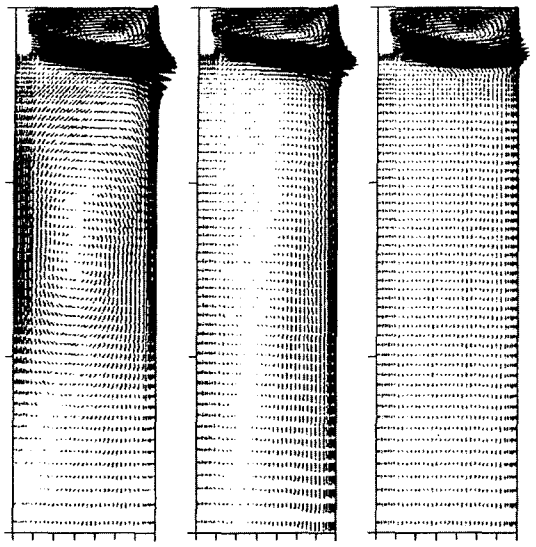

(Bz=0.0) (Bz=0.1) (Bz=0.3)

Fig. 5 Velocity vectors of the case 1 at z=0.0 m

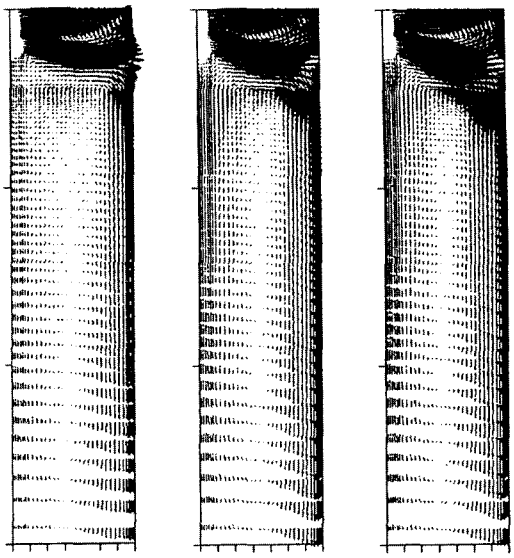

(Bz=0.1) (Bz=0.3) (Bz=0.5)

Fig. 7 Velocity vectors of the case 2 at z=0.0 m

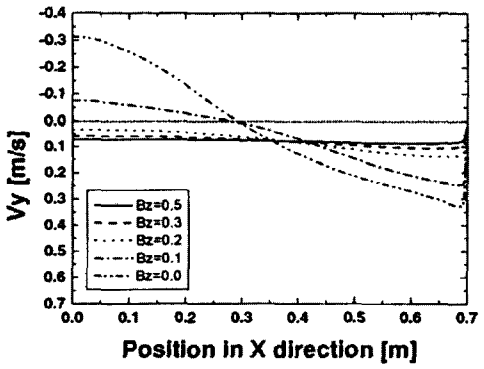

Case (1)

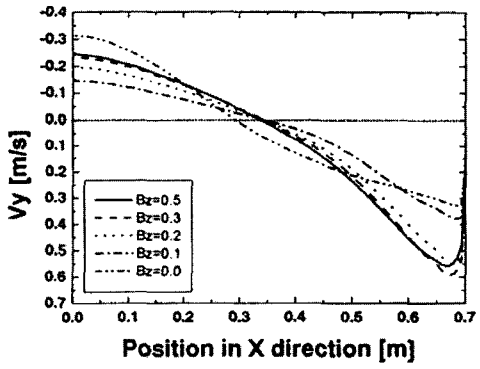

Case (2)

Fig. 6 Velocity profiles in the center of the mold (y=1.5 m and z=0.0 m)

In the center of the caster : In the case 1, with the applied magnetic field of 0.1 T, electromagnetic brake effect is not sufficiently observed. Molten steel flow is directed toward the narrow wall and it makes channeling along with the narrow wall as shown in Fig. 5. Therefore, the vorticity of downward flow is increased. With 0.3 and 0.5 T, through the stronger electromagnetic brake effect, the vorticity of vortex flow is reduced and molten steel flow becomes more uniform as shown in Fig. 6.

In the case 2, jet flow from the SEN is moved toward the narrow wall and drains down along with the narrow wall. With all of the different intensities of magnetic force, channeling occurs and downward vortex flow becomes strengthened, as shown in Fig. 7 compared with the case 1. Thus, molten flow in the center of caster is biased as shown in Fig. 6.

The outlet of the mold : In the case 1, from the center of the caster to the outlet of the mold, molten steel flow is already uniformed with applied electromagnetic effect and goes out of the caster as a uniform velocity. In the case 2, biased flow is maintained and gets out of the mold as shown in Fig. 8.

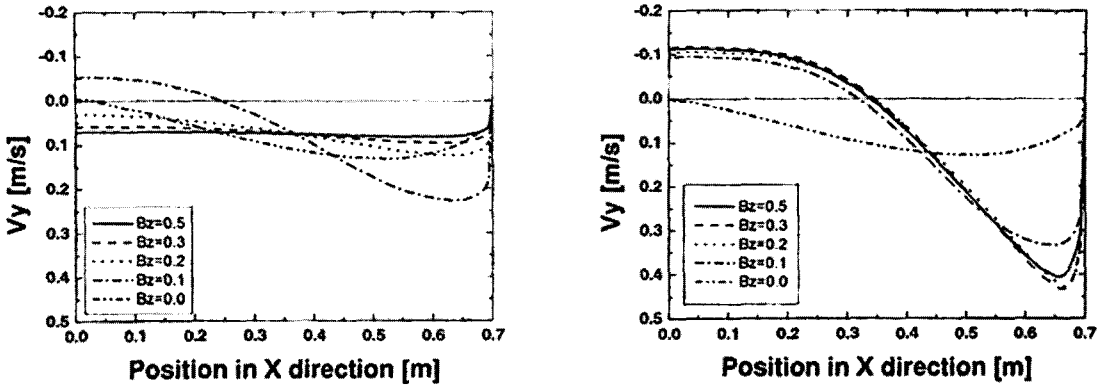

Case (1) Case (2)

Fig. 8 Velocity profiles at the outlet of the mold (y=0.285 m and z=0.0785 m)

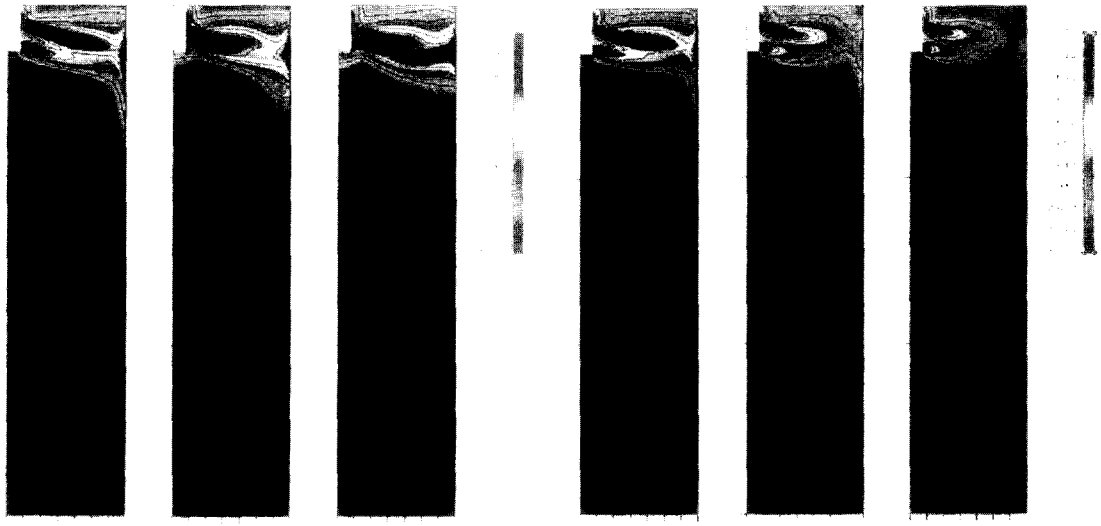

(Bz=0.0) (Bz=0.0) (Bz=0.3)

Fig. 9 The distribution of turbulent kinetic energy in the case 1

(Bz=0.1) (Bz=0.3) (Bz=0.5)

Fig. 10 The distribution of turbulent kinetic energy in the case 2

Turbulent kinetic energy in the case 1 is shown in the upper part of the SEN as shown in Fig. 9. The magnetic field in the case 1 is neither appropriate to control meniscus nor effective to reduce surface defect of steel products such as oscillation mark. Moreover, with the stronger electromagnetic force, turbulent kinetic energy also becomes more intense. In the case 2, deep penetration of turbulent kinetic energy occurs as shown in Fig. 10. It frequently drives the steel product to have internal defects such as biased solidification and inclusions of mold power or steel fragments.

4. Conclusion

Even though there have been intensive studies to adopt EMBR to continuous casting process, it is still difficult to understand molten steel flow pattern with electromagnetic effect. Molten steel flow influences directly on the quality of slabs so that it is essential to understand molten steel flow pattern to enhance the quality of slabs and the productivity of steel products.

An appropriate mathematical and physical

model are established with acceptable assumptions and analyzed numerically to understand molten steel flow pattern. Low Reynolds number $k-\varepsilon$ model and momentum equation with Lorentz force are employed. Considering y^+ less than 10 near wall regions, fine structured grids are used to analyze flow field in detail.

In this study, it is revealed that the charged place and the intensity of electromagnetic effect strongly influence on molten steel flow pattern. When suitable electromagnetic effect is applied to the mold, impingement against narrow wall is effectively suppressed, and also meniscus fluctuation and vorticity of downward flow can be controlled.

Otherwise, if electromagnetic effect would be overweighed, it could be the waste of electric power to generate electromagnetic effect and with inappropriate magnetic field, EMBR would badly influence on the molten steel flow field by channeling or biased flow, and it rather decreases the quality of steel slabs.

When a continuous casting process is designed with EMBR, the location and the intensity range of magnetic field are to be decided initially. It is very hard to modify the location of installed electromagnetic brake system after a caster is manufactured. Therefore, it should be carefully considered how to set EMBR.

This study provides numerical solutions of molten steel flows with different electromagnetic brake system to show the relation between the molten steel flow and the locations and the intensities of magnetic fields, and it would help to set EMBR system suitably and to produce high quality steel products.

References

Cha, P. R. and Yoon, J. K., 1999, "The Effect of a Uniform Direct Current Magnetic Field on the Stability of a Stratified Liquid Flux/Molten Steel System," *Metallurgical and Materials Transactions B*, Vol. 31, pp. 317~326.

Chien, K. Y., 1982, "Prediction of Channel and Boundary-Layer Flows with a Low Reynolds Number Turbulence Model," *AIAA Journal*, Vol. 20, No. 1, pp. 33~38.

Huang, X. and Thomas, B. G., 1998, "Modeling of Transient Flow Phenomena in Continuous Casting of Steel, Canadian Metallurgical Quarterly," Vol. 37, pp. 197~212.

Hwang, Y. S., Cha, P. R., Nam, H. S., Moon, K. H. and Yoon, J. K., 1997, "Numerical Analysis of the Influences of Operational Parameters on the Fluid Flow and Meniscus Shape in Slab Caster with EMBR," *ISIJ international*, Vol. 37, pp. 659~667.

Lai, K. Y. M., Salcudean, M., Tanaka, S. and Guthrie, R, I. L., 1986, "Mathematical Modeling of Flows in Large Tundish System in Steel Making," *Materials Transactions B*, Vol. 17B, pp. 449~459.

Li, B., Okane, T. and Umeda, T., 1999, "Modeling of Molten Flow in a Continuous Casting Process Considering the Effects of Argon Gas Injection and Static Magnetic-Field Application," *Metallurgical and Materials Transactions B*, Vol. 31B, pp. 1491~1503.

Park, J. P., Jeong, H. T., Sim, D. J., Chung, J. S., Kim, H. Y. and Jeong, J. Y., 1999, "The Effect of the Mold Shape on the Surface Quality of Steel Billet with Electromagnetic Casting Technology," RIST.

Seyedein, S. H. and Hasan, M., 1997, "A Three-dimensional Simulation of Coupled Turbulent Flow and Macroscopic Solidification Heat Transfer for Continuous Slab Caster," *Heat Mass Transfer International*, Vol. 40, pp. 4405~4423.

Sutton, G. W. and Sherman, A., 1986, "Engineering Magnetohydrodynamics," McGraw-Hill, New York, pp. 355~388.

Van doormaal, J. P. and Raithby, G. D., 1984, "Enhancements of the SIMPLE Method for Predicting Incompressible Fluid Flows," *Numer. Heat Transfer*, Vol. 7, pp. 147~163.

Zheng, X., Wang, Y., Li, Z. and Jin, J., 2001, "Numerical Simulation of the Temperature Field on the Electromagnetic Semi-Continuous Casting of slab," Science and Technology of Advanced Materials 2.